

Dynamical Casimir-Polder interaction between an atom and surface plasmons

Harald R. Haakh^{1,2*} and Carsten Henkel¹

¹*Institut für Physik und Astronomie, Universität Potsdam,
Karl-Liebknecht-Straße 24/25, D-14476 Potsdam, Germany*

²*Max Planck Institute for the Science of Light, Günther-Scharowski-Straße 1/24, D-91058 Erlangen, Germany*

Salvatore Spagnolo, Lucia Rizzuto, and Roberto Passante

Dipartimento di Fisica e Chimica, Università degli Studi di Palermo and CNISM, Via Archirafi 36, I-90123 Palermo, Italy

(Dated: 26 Nov 2013)

We investigate the time-dependent Casimir-Polder potential of a polarizable two-level atom placed near a surface of arbitrary material, after a sudden change in the parameters of the system. Different initial conditions are taken into account. For an initially bare ground-state atom, the time-dependent Casimir-Polder energy reveals how the atom is “being dressed” by virtual, matter-assisted photons. We also study the transient behavior of the Casimir-Polder interaction between the atom and the surface starting from a partially dressed state, after an externally induced change in the atomic level structure or transition dipoles. The Heisenberg equations are solved through an iterative technique for both atomic and field operators in the medium-assisted electromagnetic field quantization scheme. We analyze in particular how the time evolution of the interaction energy depends on the optical properties of the surface, in particular on the dispersion relation of surface plasmon polaritons. The physical significance and the limits of validity of the obtained results are discussed in detail.

PACS numbers: 34.35.+a – interactions of atoms with surfaces; 42.50.Nn – quantum optical phenomena in conducting media; 73.20.Mf – surface plasmons

A striking feature of the quantum nature of the electromagnetic field is the existence of a vacuum energy and of zero-point fluctuations. Field fluctuations have observable effects such as the Lamb shift, spontaneous emission, Casimir-Polder forces, and the Casimir effect [1–4]. In particular, Casimir-Polder forces are long-range electromagnetic interactions between neutral polarizable atoms or molecules (van der Waals interaction), or between an atom and a macroscopic object, that arise from the zero-point fluctuations of the electromagnetic field and matter [5–7]. Their prediction is arguably one of the most important results of quantum electrodynamics. The macroscopic counterpart of the Casimir-Polder forces is the Casimir effect, predicting an attractive force between two parallel uncharged plates [8]. The relation between the Casimir effect and Casimir-Polder forces has been extensively investigated in the literature, highlighting fundamental properties such as the nonadditivity [1, 9] and fluctuations (see Ref. [10] and references therein). Experiments conducted from the second half of the nineties to now, have incontrovertibly shown the reality of these rather counterintuitive effects [3, 4, 11, 12]. It is now recognized that the Casimir effect plays an important role in the operation of micro- and nano-electromechanical devices (MEMS and NEMS) [3, 4, 13]. In particular, the research of experimental setups that allow for a modulation of the intensity or the sign of the force is of great interest as it may help to prevent the jamming (‘stiction’) of such machinery due to attractive forces, leading to the

breakdown of the device. In the field of miniaturized atom traps, the control over the Casimir-Polder attraction is desirable to achieve stable trapping at distances below one micron[14].

Recently, great attention has been paid to the so-called dynamic Casimir effect. Here, theory predicts that forcing a plate to a rapid mechanical oscillatory motion leads to the generation of real photons from the electromagnetic vacuum state (see Ref. [15] and references therein). The phenomenon has not yet been confirmed by experiments directly. In fact, for a measurable number of real photons to be produced, the wall must oscillate at frequencies that are not experimentally accessible, yet. However, alternative schemes for the realization of the dynamic Casimir effect have been proposed. For example, the mechanical movement of the wall may be replaced by a suitable modulation of the optical properties of one of the surfaces [16–18] or of the optical path length of a cavity [19]. Analogous effects have been recently observed in the context of superconducting circuits [20] and in trapped Bose-Einstein condensates [21].

The microscopic counterpart of the dynamic Casimir effect is the dynamic Casimir-Polder effect [22–25]. Recent work has studied the dynamic Casimir-Polder forces between an atom and a perfectly reflecting plate [23–25]. It has been shown that after a sudden change of the atom-field interaction parameters, the force exhibits oscillations in time and can be attractive or repulsive depending on time and the atom-wall distance. This is at variance with the stationary atom-plate Casimir-Polder force for a ground-state atom, which is generally attractive at all distances between the atom and the plate. A description in terms of a perfectly reflecting plate obviously neglects

*Electronic address: harald.haakh@mpl.mpg.de

the dynamics of charge transport [4, 26] and does not take into account phenomena such as UV transparency and surface-mode excitations. In fact, these are known to play a crucial role in the near-field of conducting surfaces, and in particular in short-distance atom-surface interactions [27–32]. We therefore generalize previous work on the dynamic Casimir-Polder interaction from the case of perfectly reflecting surfaces to allow for the description of an arbitrary surface material in terms of optical response functions.

More specifically, we investigate the dynamic (i.e., time-dependent) Casimir-Polder force between a neutral atom and a real surface and follow its relaxation towards a new equilibrium quantum state (“atom dressing”). Such a situation can occur when a parameter involved in the atom-field coupling (such as the atomic transition frequency or the atom-plate distance) is suddenly modified [24, 25]; in this case a time dependence of the force is expected. We shall consider two different initial conditions for the system: an initially bare atom, and a partially dressed one [33, 34]. The latter scenario occurs if a nonadiabatic change of the atomic properties is externally induced, for example by an external electric field. We investigate the time-dependent atom dressing and the resulting atom-surface Casimir-Polder potential, and discuss how the physical properties of the surface material can influence the time dependence of the Casimir-Polder force, in particular its intensity and sign. This is expected, because the surface can respond to the field generated by the atom and participate in the dynamics of the system, in particular through surface excitations. The results obtained in the two cases are compared with those already obtained in the literature for the limiting case of an ideal reflecting plate. We find that also in the case of a general surface, the dynamic Casimir-Polder energy exhibits oscillations in time, yielding a transient repulsive force, and that asymptotically settles to its stationary value. Combining time-dependent perturbation theory with the matter-assisted field approach [35–39], we evaluate the effects on the dynamic dressing caused by the metallic surface with a focus on the role of surface excitations. The formalism makes it possible to explore realistic situations close to those experimentally achievable, and it may also allow us to determine whether specific physical properties of the wall can be used to control the atomic dressing time and hence the intensity or the sign of the Casimir-Polder force.

The paper is organized as follows. In Sec. I, we give a brief review of the formalism used to calculate the time evolution of the atom-surface potential. The influence of material properties and surface mode excitations on the dynamic atom-surface interaction is considered in Sec. II. In Sec. III, we investigate the effect of a sudden change of the atomic properties on the dynamic atom-wall Casimir-Polder potential. Finally, in Sec. IV, we summarize and discuss the physical features and limits of validity of our results. Technical details related to the electromagnetic surface response (Green tensor) are

given in the Appendix.

I. DYNAMIC DRESSING OF AN INITIALLY BARE ATOM

Let us consider a neutral atom interacting with the quantum electromagnetic field in the presence of a real surface of arbitrary material. The Hamiltonian of a polarizable atom interacting with the matter-assisted electromagnetic field in the multipolar coupling scheme and dipole approximation is [35–39]

$$\begin{aligned} H &= H_F + H_A + H_{AF} \\ &= \int_0^\infty d\omega \int d^3x \hbar\omega \mathbf{f}^\dagger(\mathbf{x}, \omega) \cdot \mathbf{f}(\mathbf{x}, \omega) \\ &\quad + \hbar\Omega S_z - \hat{\mathbf{d}} \cdot \mathbf{E}(\mathbf{r}), \end{aligned} \quad (1)$$

where, for simplicity, the atom is described as a two level system, located at \mathbf{r} and characterized by a single Bohr frequency Ω and pseudospin-operators S_\pm, S_z [2]. The operator

$$\hat{\mathbf{d}} = \mathbf{d}(S_+ + S_-), \quad (3)$$

is the dipole moment, the vector \mathbf{d} contains its transition matrix elements, assumed real, and takes the role of a coupling constant. Moreover, $\mathbf{f}, \mathbf{f}^\dagger$ are generalized bosonic matter-field operators with commutation relations $[\mathbf{f}(\mathbf{x}, \omega), \mathbf{f}(\mathbf{x}', \omega')] = \delta(\mathbf{x} - \mathbf{x}')\delta(\omega - \omega')$. The electric field operator \mathbf{E} is expressed through the electric Green’s tensor $\mathcal{G}_{mn}(\mathbf{x}, \mathbf{x}', \omega)$ (see Appendix A for the explicit form) and reads [37],

$$\begin{aligned} E_m(\mathbf{r}, t) &= \int_0^\infty d\omega \int d^3\mathbf{x} \sqrt{\frac{\hbar}{\pi}} \varepsilon_0 \text{Im} \varepsilon(\mathbf{x}, \omega) \\ &\quad \times [i\mathcal{G}_{mn}(\mathbf{r}, \mathbf{x}, \omega) f_n(\mathbf{x}, t; \omega) + h.c.] . \end{aligned} \quad (4)$$

Throughout this work, Einstein sums over double spatial indices are implied. The presence and the physical properties of the surface are encoded in the Green’s tensor via reflection amplitudes and the dielectric function of the medium, $\varepsilon(\mathbf{x}, \omega)$. When we make calculations for a specific surface model, we shall consider the simplest case of a nonmagnetic material with finite conductivity, that is the Drude model with a dielectric function [40]

$$\varepsilon(\omega) = 1 - \frac{\omega_p^2}{\omega(\omega + i\gamma)}, \quad \mu(\omega) = 1 \quad (5)$$

with ω_p the plasma frequency and γ the dissipation rate.

In the vicinity of a body of arbitrary dispersive and dissipative material, the excitations of the electromagnetic field cannot be separated from the excitations of the matter. This nonseparability is taken into account in the matter-assisted field approach [36–38] by the generalized bosonic operators $\mathbf{f}, \mathbf{f}^\dagger$. Eq. (4) therefore generalizes a mode decomposition, necessary for the time-dependent perturbation theory which we will now employ.

Following the procedure already used in previous works [24, 25], the equation of motion for a general atomic or field operator A is calculated from the Heisenberg equations. This leads to a series expansion $A(t) = \sum_n A^{(n)}(t)$, where n indicates the power of the coupling constant. Up to the first order in the coupling, we find

$$S_+^{(0)}(t) = S_+^{(0)}(0)e^{i\Omega t}, \quad (6)$$

$$S_+^{(1)}(t) = \frac{2i}{\hbar}e^{i\Omega t} \int_0^t dt' S_z^{(0)}(0) \mathbf{d} \cdot \mathbf{E}^{(0)}(t') e^{-i\Omega t'}, \quad (7)$$

and

$$\mathbf{f}^\dagger(\mathbf{x}, t; \omega) = \mathbf{f}^\dagger(\mathbf{x}, 0; \omega) e^{i\omega t}, \quad (8)$$

$$f_n^\dagger(\mathbf{x}, t; \omega) = e^{i\omega t} \sqrt{\frac{\varepsilon_0}{\hbar\pi}} \text{Im} \varepsilon(\omega) d_m \mathcal{G}_{mn}(\mathbf{x}, \mathbf{r}, \omega) \times \left[S_+^{(0)}(0) F(\Omega - \omega, t) + S_-^{(0)}(0) F(-\Omega - \omega, t) \right]. \quad (9)$$

We stress that we do not impose the rotating wave approximation (RWA) so that Eq. (9) contains both resonant (first term) and antiresonant (second term) contributions. The time-dependence is abbreviated by

$$F(\omega, t) = \int_0^t dt' e^{i\omega t'} = \frac{e^{i\omega t} - 1}{i\omega}. \quad (10)$$

The solutions obtained above are operator equations, valid for any initial state.

We now consider a specific initial state at $t = 0$ for the system. In particular, we consider a ground-state atom at zero temperature. The time-dependent Casimir-Polder potential is obtained from the energy shift $U(z, t) = \frac{1}{2} \langle H_{AF}(t) \rangle$ and, by symmetry, can depend only on the distance z between the atom and the surface. Our analysis is restricted to the second order in the coupling constant \mathbf{d} and mean values are taken with respect to the bare ground-state $|\text{vac}, \downarrow\rangle$, so that

$$U(z, t) \approx -\frac{1}{2} \langle \hat{\mathbf{d}}^{(0)} \cdot \mathbf{E}^{(0)} \rangle - \frac{1}{2} \langle \hat{\mathbf{d}}^{(0)} \cdot \mathbf{E}^{(1)} \rangle - \frac{1}{2} \langle \hat{\mathbf{d}}^{(1)} \cdot \mathbf{E}^{(0)} \rangle. \quad (11)$$

It is clear that the first term is off-diagonal in the spin basis and does not contribute. The remaining terms can be evaluated by using the identity

$$\text{Im} \mathcal{G}_{ij}(\mathbf{r}_1, \mathbf{r}_2, \omega) = \int d^3\mathbf{x} \varepsilon_0 \text{Im} [\varepsilon(\omega, \mathbf{x})] \mathcal{G}_{ik}(\mathbf{r}_1, \mathbf{x}, \omega) \mathcal{G}_{jk}^*(\mathbf{x}, \mathbf{r}_2, \omega), \quad (12)$$

which is a known property of the electromagnetic Green's tensors contained already in Maxwell's equations [35, 41, 42]. Besides, from the reciprocity principle we have $\mathcal{G}_{ij}(\mathbf{r}, \mathbf{r}', \omega) = \mathcal{G}_{ji}(\mathbf{r}', \mathbf{r}, \omega)$ and for hermitean fields $\mathcal{G}_{ij}(\mathbf{r}, \mathbf{r}', -\omega) = \mathcal{G}_{ij}^*(\mathbf{r}, \mathbf{r}', \omega)$ (with $\omega \in \mathbb{R}$). Thus,

$$-\frac{1}{2} \langle \hat{d}_m^{(0)} E_m^{(1)}(\mathbf{r}, t) \rangle = -id_m d_n \int_0^\infty \frac{d\omega}{2\pi} \text{Im} \mathcal{G}_{mn}(\mathbf{r}, \mathbf{r}, \omega) \left[e^{-i(\Omega+\omega)t} F(\Omega + \omega, t) - e^{-i(\Omega-\omega)t} F(\Omega - \omega, t) \right] \quad (13)$$

$$-\frac{1}{2} \langle \hat{d}_m^{(1)} E_m^{(0)}(\mathbf{r}, t) \rangle = +id_m d_n \int_0^\infty \frac{d\omega}{2\pi} \text{Im} \mathcal{G}_{mn}(\mathbf{r}, \mathbf{r}, \omega) \left[e^{i(\Omega+\omega)t} F(-\Omega - \omega, t) - e^{-i(\Omega-\omega)t} F(\Omega - \omega, t) \right]. \quad (14)$$

Summing up Eqs. (13) and (14), the last terms with a pole at $\omega = \Omega$ cancel out each other and the energy shift at second order becomes

$$U(\mathbf{r}, t) = -d_m d_n \int_0^\infty \frac{d\omega}{2\pi} \text{Im} \mathcal{G}_{mn}(\mathbf{r}, \mathbf{r}, \omega) \times \left(\frac{2}{\Omega + \omega} - \frac{2 \cos[(\Omega + \omega)t]}{\Omega + \omega} \right). \quad (15)$$

From now on, we will use the shorthand

$$G(\omega) \equiv d_m d_n \mathcal{G}_{mn}(\mathbf{r}, \mathbf{r}, \omega) \quad (16)$$

for the projected single-point Green's tensor. The previous Eq. (15) is easily recognized as the equivalent of Eq. (13) of Ref. [24] and it is manifestly real. In order to distinguish the static contribution from the time-dependent term, we separate the two terms in the second line of Eq. (15) and define

$$U(\mathbf{r}, t) = U_{\text{stat}}(\mathbf{r}) + U_{\text{dyn}}(\mathbf{r}, t). \quad (17)$$

The system is unperturbed at $t = 0$ and its evolution must be continuous so that $U(\mathbf{r}, 0) = 0$. The correction U_{dyn} describes the transient dressing dynamics and averages to zero in the stationary limit $t \rightarrow \infty$, due to the oscillatory integrand. In this limit, we recover the stationary Casimir-Polder potential U_{stat} given in Ref. [43]. Note that expression (15) does not depend any more explicitly on a bulk property like $\text{Im} \varepsilon(\mathbf{x}, \omega)$, but only on the total Green's tensor above the surface. This allows for the calculation of the time-dependent energy shift of an atom in a rather general setting, and remains valid even in cases where the microscopic details of the surface response are completely ignored, as in the limit case of a perfect reflector. In the following we shall use expression (15) to obtain the dynamic atom-wall Casimir-Polder potential, for an atom placed near a planar surface described by a dielectric or metallic half-space.

As a first step, we now consider the case of ideal reflec-

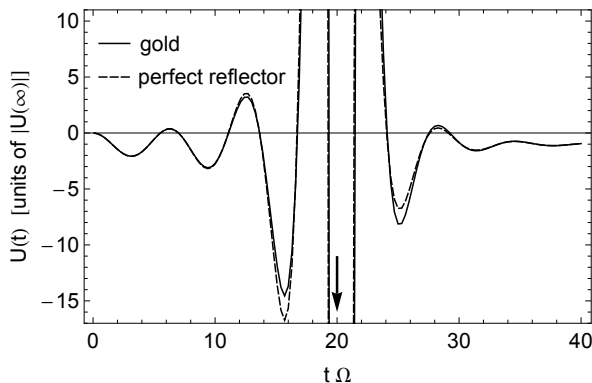


FIG. 1: Time dependent energy shift near a gold surface (solid line) and near a perfect reflector (dashed line). Parameters for gold are $\hbar\omega_p = 8.9\text{eV}$, $1/\gamma = 19\text{fs}$. The atomic transition frequency corresponds to the 780nm line of rubidium 85 ($\Omega = 0.18\omega_p$), and the atom-surface distance is $z = 10c/\Omega = 1.2\mu\text{m}$. At the signal-transit time $\Omega t = 20$, indicated by the arrow, the reflected light cone reaches the atom. On this scale, the curve obtained from the Drude model for gold and from its lossless limit ($\gamma \rightarrow 0$), respectively, cannot be distinguished.

tor; the dynamic atom-wall Casimir-Polder energy has been already investigated in Refs. [24] and provides a convenient cross-check. The two-level atom is assumed to be isotropically polarizable, so that $d_m d_n = \frac{1}{3}|d|^2 \delta_{mn}$. In the limit of a perfect reflector (reflection coefficients $r_p = -r_s = 1$), the single-point Green's tensor may be expressed through a spatial differential operator \mathcal{D} :

$$G(\omega) \mapsto \frac{|d|^2}{3} \mathcal{D} e^{2i\omega z/c}, \quad (18)$$

$$\mathcal{D} = \lim_{\alpha \rightarrow 1} \frac{1}{16\pi\epsilon_0 z^3} \left(2 - 2\frac{\partial}{\partial\alpha} + \frac{\partial^2}{\partial\alpha^2} \right). \quad (19)$$

We immediately obtain

$$U(z, t) = -\frac{|d|^2}{3} \int_0^\infty \frac{d\omega}{2\pi} \mathcal{D} \sin(2\alpha z\omega/c) \times \frac{2 - 2\cos[(\Omega + \omega)t]}{\Omega + \omega}, \quad (20)$$

where z is the atom's distance with respect to the plate. This equation corresponds to Eq. (13) of Ref. [24]. There, an explicit expression for the force was obtained in terms of cosine and sine integral functions. A numerical evaluation of Eq. (20), giving the time-dependent energy shift of an atom near a perfect reflector, is shown in Fig. 1 (dashed line). Important features of Fig. 1 have already been discussed in Refs. [23, 24]. It is shown that the dynamic atom-wall Casimir-Polder energy, exhibits oscillations in time, yielding transient repulsive force and that in the asymptotic limit it settles to a stationary value. Strong effects set in when the atom begins to 'see' its own mirror image, precisely at the signal-transit time $t = 2z/c$, when the reflected light cone reaches the atom.

As explained in Refs. [23, 24], the nontrivial divergence in the radiation reaction at this moment can be traced back to the point dipole approximation [44] and to assuming the atom initially bare [34]. The energy shift shows a precursor for $t < 2z/c$ because the atom starts to evolve unitarily under the full Hamiltonian, i.e. it couples instantaneously to the fluctuating field [24].

In the next Section we shall consider in detail the dressing problem and the atom-wall Casimir-Polder interaction in the case of a general surface, and we discuss in detail the role of the physical properties of the surface on the dynamic atomic dressing.

II. MATERIAL PROPERTIES AND SURFACE MODE EXCITATIONS

Let us now consider an atom near a surface with an arbitrary linear electromagnetic response. Here, the evaluation of Eq. (15) is not straightforward because of the oscillating integrand. It is therefore very useful to perform an analytic continuation to complex frequencies as shown in the following subsection. We take advantage of the fact that the Green function $G(\omega)$ is analytic for complex ω in the upper half-plane, as it must for a retarded response.

A. Imaginary frequency representation

The static Casimir-Polder potential is often written as an integral over imaginary frequencies. To achieve this form, we use the relation $2i\text{Im} G(\omega) = G(\omega) - G(-\omega)$ ($\omega \in \mathbb{R}$) and integrate along contours I and II in Fig. 2. Using the fact that the surface becomes transparent as $|\omega| \rightarrow \infty$ in the upper half-plane, we recover the expression for the static shift reported in Ref. [43],

$$U_{\text{stat}}(z) = -\int_0^\infty \frac{d\xi}{2\pi} G(i\xi) \frac{2\Omega}{\Omega^2 + \xi^2}. \quad (21)$$

The analytic properties of the dynamic part are more subtle. Expressing the cosine in Eq. (15) as the real part of a complex exponential, we find

$$U_{\text{dyn}}(z, t) = -\text{Re} i e^{i\Omega t} \int_0^\infty \frac{d\omega}{2\pi} G(\omega) \frac{e^{i\omega t}}{\omega + \Omega} + \text{Re} i e^{i\Omega t} \int_{-\infty}^0 \frac{d\omega}{2\pi} G(\omega) \frac{e^{-i\omega t}}{-\omega + \Omega}. \quad (22)$$

In the first line, the integrand is regular in the upper complex half-plane and can be shifted to the positive imaginary axis (contour I in Fig. 2). Two different cases must be considered for the second integral, according to times before or after the transit time $2z/c$. As can be easily inferred from the expressions obtained in the Appendix, the asymptotic behavior of the Green's tensor for large values of $|\omega|$ is of the form $G(z, \omega) e^{-i\omega t} = e^{i\omega(2z/c-t)} g(z, \omega)$.

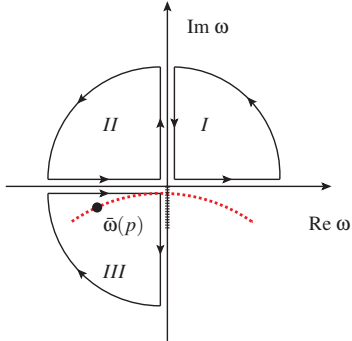


FIG. 2: (Color online) Integration contours for the analytic continuation. In the range $\text{Re } \omega > 0$, convergence is always guaranteed for the first integral in (22) in the upper half-space (contour I). For the second integral in (22): outside the reflected light cone ($ct < 2z$), the integration contour $\text{Re } \omega < 0$ is closed in the upper complex plane (contour II); inside the light cone ($ct > 2z$), contour III applies, avoiding a possible branch-cut along negative imaginary axis (hatched line). The red dotted line symbolizes the surface-plasmon resonances at $\bar{\omega}(p)$, contributing a single isolated pole at a given value of momentum p parallel to the surface.

If $ct < 2z$, i.e. before the signal transit time, the integral converges in the upper complex half-plane; if $ct > 2z$, i.e. afterwards, it converges in the lower complex half-plane. The integrals can therefore be evaluated using the contours II and III in Fig. 2, respectively. Note that for ground-state atoms, the poles in Ω are never inside the contour, so that there are no contributions from atomic resonances. The time-dependent potential is

$$\begin{aligned}
 U_{\text{dyn}}(z, t) = & \text{Re } e^{i\Omega t} \left[\int_0^\infty \frac{d\xi}{2\pi} G(i\xi) \frac{e^{-\xi t}}{i\xi + \Omega} \right. \\
 & + \int_0^\infty \frac{d\xi}{2\pi} G(i\xi) \frac{e^{\xi t}}{-i\xi + \Omega} \theta(2z - ct) \\
 & - \int_{-\infty}^0 \frac{d\xi}{2\pi} G(i\xi) \frac{e^{\xi t}}{-i\xi + \Omega} \theta(ct - 2z) \\
 & \left. + i \oint_{III} \frac{d\omega}{2\pi} G(\omega) \frac{e^{-i\omega t}}{-\omega + \Omega} \theta(ct - 2z) \right]. \quad (23)
 \end{aligned}$$

This expression is a central result of the present work. The imaginary frequency integrals are sufficiently well-behaved to be evaluated numerically using a general Green's tensor. The last term in Eq. (23) will be denoted by ΔU_{res} and includes the transient contribution due to material excitations (poles of the Green's tensor), as we shall discuss in detail in the next subsection.

To get rapidly converging expressions, we have so far written all integrals over retarded Green's tensors (positive frequency arguments) which are analytic in the upper complex plane. However, from the form of Eq. (22) only odd-parity terms of the Green's tensor contribute. In fact we may obtain equivalent results by considering $[G(\omega) - G(-\omega)] e^{i\omega t}$ a meromorphic function that con-

verges along the contour I for $t > 2z/c$ but contains a pole in the upper half-plane.

A numerical evaluation of the total time-dependent energy shift obtained from the imaginary frequency formulation of Eqs. (22) and (23) is compared in Fig. 1 to the results for a perfect reflector. Clearly, for this distance in the far zone ($z \gg c/\Omega$), the dependence on the material properties is relatively weak. This is because in this regime, the electromagnetic field, except very close to the reflected light cone, is mediated by propagating photonic modes with low frequency: for these modes the perfect reflector provides a reasonable boundary condition even for a real material. In fact, this can be shown directly for the Green's tensor at large distances above a general metal [45]. As shown in Fig. 1, the potentials obtained for a perfect reflector and for a gold surface differ strongest at times close to the signal transit time: at this instant, the response is dominated by high-energy modes, and a gold surface shows a cutoff above its plasma frequency.

B. Surface-plasmon contribution

The matter-assisted photon modes (plasmons or polaritons) near a real material are encoded in the analytic structure of the Green function $G(\omega)$. In particular surface excitations play an important role [28, 46, 47]. They appear as poles and singularities of $G(\omega)$ in the lower half-plane $\text{Im } \omega < 0$. For times $t > 2z/c$, they contribute to the time-dependent potential, as can be seen from the last integral in Eq.(23). Different types of polaritons can be identified from the integral representation of $G(\omega)$ given in Eq.(A3) of the Appendix. Isolated poles of the reflection coefficients correspond to surface plasmon modes. The dielectric function $\varepsilon(\omega)$ gives rise to bulk plasmons in the high-frequency range $\omega > \omega_p$.

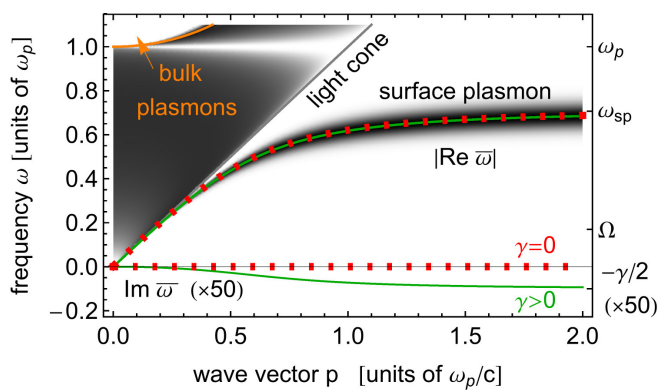


FIG. 3: (Color online) Surface plasmon dispersion relation $\bar{\omega}(p)$ in the Drude model for gold (green solid curves, parameters as in Fig. 1). Red dotted curves correspond to the lossless limit $\gamma \rightarrow 0$ of Eq. (25). The plasmonic frequency scales ω_p and ω_{sp} , and the atomic resonance frequency Ω are indicated for the parameters of Fig.1. The gray scale background gives $|\text{Im } r_p(\omega, p)|$.

A conducting medium features additional diffusive low-frequency excitations ('eddy currents') connected with branch-cut discontinuities along the negative imaginary axis. Since the latter have a minor impact in electric-dipole coupling [45, 48, 49], we focus in the following on the surface excitations.

A surface described by the Drude model of Eq. (5) carries a single surface plasmon given by a pole of the reflectivity in p-polarization

$$\varepsilon(\omega)\kappa(\omega, p) + \kappa_m(\omega, p) = 0, \quad (24)$$

where the notation of Appendix A is used. The solution $\bar{\omega}(p)$ is shown in Fig. 3 and will be used for numerical evaluations in Sec. II E. In the general case, the analytic form is not very instructive. However, a simple expression is obtained in the lossless limit $\gamma \rightarrow 0$. Here, the relevant branch of the surface-plasmon dispersion relation inside the contour III of Fig. 2 is [47]

$$\bar{\omega}(p) = -\sqrt{\omega_{\text{sp}}^2 + c^2 p^2} - \sqrt{\omega_{\text{sp}}^4 + c^4 p^4} - i0^+, \quad (25)$$

$$\bar{\kappa}(p) = \sqrt{\omega_{\text{sp}}^4/c^4 + p^4 - \omega_{\text{sp}}^2/c^2}, \quad (26)$$

where the surface-plasmon frequency $\omega_{\text{sp}} = \omega_p/\sqrt{2}$ is the asymptotic value at large wave vectors and $\bar{\kappa}(p)$ governs the decay of the surface mode outside the material. The surface plasmon-polariton is an evanescent wave, i.e. its dispersion relation lies below the light cone [$\bar{\omega}(p) < pc$, see Fig. 3]. Fig. 3 illustrates that Eq. (25) provides a very good approximation to the resonance frequency $\text{Re } \bar{\omega}$ of a good conductor ($\gamma \ll \omega_p$). Of course, it cannot account adequately for plasmon damping ($\text{Im } \bar{\omega}$). We will see that damping plays a role at short distances (Sec. II E) and gives the otherwise monochromatic dispersion relation a finite width [50].

Using the integral form (A3) of the electric Green's tensor and the previous expression for the plasmon dispersion, it is possible to calculate separately the resonant contribution in Eq. (23), similar to previous approaches in the static case [27]. The integrals over wave vectors and frequency are interchanged and the atom is assumed to be isotropically polarizable, so that ($t > 2z/c$)

$$\begin{aligned} \Delta U_{\text{res}}(z, t) &= \frac{|d|^2}{12\pi\varepsilon_0} \text{Re} \int_0^\infty dt e^{i\Omega t} \int_0^\infty dp \oint_{\text{III}} \frac{d\omega}{2\pi} \frac{e^{-i\omega t - 2\kappa z}}{-\omega + \Omega} \frac{p}{\kappa} \\ &\times \left[\frac{\omega^2}{c^2} r_s(\omega, p) + r_p(\omega, p) \left(\frac{\omega^2}{c^2} + 2\kappa^2 \right) \right]. \end{aligned} \quad (27)$$

The surface plasmon arises from a single isolated pole at $\omega = \bar{\omega}(p)$ which is located inside the contour due to its negative imaginary part. In the lossless limit of Eq. (25), this is achieved by the infinitesimal imaginary shift. We calculate the residue from a series expansion of the denominator of the r_p coefficient,

$$R_p(\omega, p) = \frac{\varepsilon(\omega)\kappa - \kappa_m}{\frac{d}{d\omega}[\varepsilon(\omega)\kappa + \kappa_m]}. \quad (28)$$

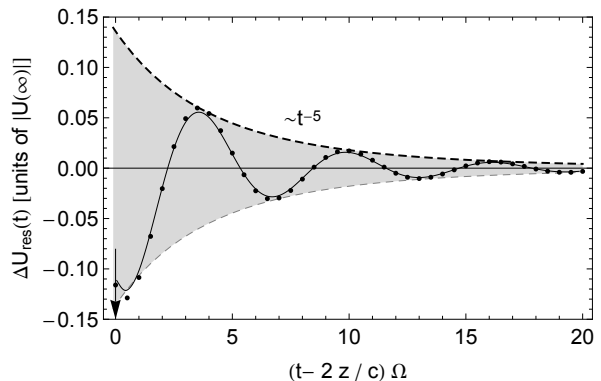


FIG. 4: Resonant surface mode contribution ΔU_{res} [Eq. (29)] to the atom-surface dressing near a gold surface (solid line, parameters as in Fig. 1). Dots give the lossless limit $\gamma \rightarrow 0$). Relatively large atom-surface distance: $z = 10c/\Omega$. The contribution sets in only after the signal-transit time $t = 2z/c$. The envelope shows good agreement with the t^{-5} power law expected at this distance

Using the residue theorem for the clockwise contour, the contribution due to the surface plasmon, present at $t > 2z/c$, is

$$\begin{aligned} \Delta U_{\text{res}}(z, t) &= \frac{|d|^2}{12\pi\varepsilon_0} \text{Re} \frac{e^{i\Omega t}}{2} \int_0^\infty dp \frac{p}{\bar{\kappa}(p)} \\ &\times \frac{e^{-i\bar{\omega}(p)t - 2\bar{\kappa}(p)z}}{-\bar{\omega}(p) + \Omega} \left(2p^2 - \frac{\bar{\omega}^2(p)}{c^2} \right) R_p(\bar{\omega}(p), p). \end{aligned} \quad (29)$$

This resonant contribution to the atom-surface interaction is plotted in Fig. 4, normalized to $U(\infty)$ near a gold surface. The full complex dispersion relation is nearly indistinguishable from the lossless limit discussed above.

C. Large distance

The data of Fig. 4 are calculated for a distance larger than the atomic resonant wavelength (retarded regime). The surface modes then contribute only a minor fraction of the total dynamic Casimir-Polder energy. Their contribution is a transient effect and decays quickly in time due to the wide frequency range in the integral (17). In the far field, where small values of p contribute and where the plasmon dispersion relation approaches the light cone, even a dissipative medium provides very little damping (cf. Fig. 3). The relaxation is, therefore, clearly not a dissipative effect but rather due to the dephasing between spectral components, because of the broad bandwidth of the plasmon dispersion covering the interval $|\bar{\omega}(p)| \in [0; \omega_{\text{sp}}]$.

We get some insight by studying the envelope of the resonant potential in the retarded regime. The relevant contributions to the integral in Eq. (29) stem from low-momentum modes near the light cone. We change from p to $\bar{\omega}$ as integration variable using the dispersion relation [Eqs. (25), (26)] and expand the integrand for small

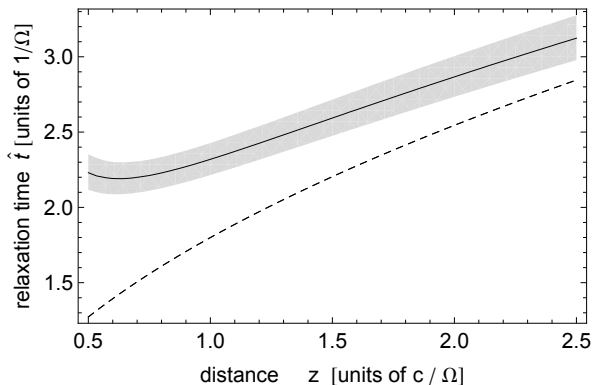


FIG. 5: Time scale for the transient atom-surface dressing vs. distance. Parameters are those of a rubidium atom near a gold surface, as in Fig. 1. Shaded band with solid line: numerically calculated $1/e$ decay time of the dynamic Casimir-Polder energy, with 5% error margins. Dashed line: estimate $\tau\pi[z/(\omega_{\text{sp}}c)]^{1/2}$ derived in the main text, with fitting parameter $\tau = 1.1$. At short distance the plasmon spectrum becomes monochromatic and losses limit the relaxation time, see Sec. II E.

frequencies. This gives a power law $\bar{\omega}^4$ and therefore an algebraic decay $\propto t^{-5}$ at large times. The good agreement between this power law and the numerical solution is shown in Fig. 4.

D. Intermediate distance

At intermediate distances $c/\omega_p < z < 2c/\Omega$, the time scale of the decay can be estimated from the exponential in the integral in Eq. (29), the rest of the integrand being a well-behaved function that vanishes as $p \rightarrow 0$ and is polynomial at infinity. From the distance-dependent part of the integrand, only values of p such that $\bar{\kappa}(p)z < 1$ are relevant, so that $p < \hat{p} = (z^{-4} + \omega_{\text{sp}}^2/c^2 z^2)^{1/4}$. If the oscillating exponential covers much more than half a period in this range of p , both the real and imaginary part of the integral will eventually be small on average. The typical timescale on which the resonant contribution decays is, therefore, given by $\hat{t} = \tau\pi/\bar{\omega}(\hat{p})$, with τ a coefficient of order unity. For atom-surface separations beyond the plasma wavelength, the time scale can be roughly estimated by $\hat{t} \approx \tau\pi[z/(\omega_{\text{sp}}c)]^{1/2}$, the geometric mean between the plasma period and the signal-transit time.

Fig. 5 compares this estimate with a numerical solution. At short distances, large momenta p become relevant and the above approximation does no longer apply. The surface spectrum then strongly peaks at the plasmon resonance. We will see in the following Section that the relaxation of the dynamic Casimir-Polder interaction slows down significant and is limited by Ohmic losses in the bulk.

E. Near-field dressing

We now consider short distances, $z \ll c/\omega_p \ll c/\Omega$, where the surface-mode contribution is dominant. Dissipative properties of the surface are crucial in the near field and we assume the Drude metal of Eq. (5) allowing for a finite damping rate γ . As a result, the surface modes broaden as shown in Fig. 3.

At frequencies connected with electric dipole transitions, this near field regime corresponds to atom-surface separations smaller than the normal skin depth of the metallic surface. Here, an asymptote of the reflected electric Green's tensor is obtained from an expansion for large in-plane wavevectors $p \gg \omega_p/c, \omega/c$

$$G(z, \omega) \approx \frac{d^2 + d_z^2}{32\pi\epsilon_0 z^3} r_p(\omega), \quad (30)$$

$$r_p(\omega) \approx \frac{\epsilon(\omega) - 1}{\epsilon(\omega) + 1}. \quad (31)$$

The expression can be analytically continued to complex frequencies and is well-behaved along the whole imaginary axis. From here and Eq. (21) the well-known static van der Waals-Casimir-Polder potential follows immediately. We recall that for an isotropically polarizable atom near a perfectly reflecting surface we have $U_{\text{stat}} = -|d|^2/(48\pi\epsilon_0 z^3)$, whereas the potential is reduced by a factor $\omega_{\text{sp}}/(\Omega + \omega_{\text{sp}}) \approx 0.8$ for the Drude parameters of gold and the atomic transition considered in the numerics [43].

In the near field, retardation can be neglected and the signal-transit time coincides with $t = 0$. To obtain the time dependent potential from Eq. (23), we must again consider the isolated pole of the near field Green's tensor inside contour III of Fig. 2, given approximately by

$$\bar{\omega}(\infty) = -\omega_{\text{sp}} - i\frac{\gamma}{2}, \quad (32)$$

up to small corrections $\mathcal{O}(\gamma^2/\omega_{\text{sp}}^2)$. This corresponds to the asymptotically flat regime of the surface mode (cf. Fig. 3). The relevant residue of r_p [Eq.(28)] is now $R_p(\bar{\omega}(\infty), \infty) = 1$ and results in a resonant contribution

$$\Delta U_{\text{res}}(z, t) = \frac{|d|^2 \omega_{\text{sp}}}{48\pi\epsilon_0 z^3} \text{Re} \left[\frac{e^{i(\Omega - \bar{\omega}(\infty))t}}{\Omega - \bar{\omega}(\infty)} \right]. \quad (33)$$

This cancels exactly with the static Casimir-Polder potential for $t \rightarrow 0$. The physical reason is that the static potential, too, originates mainly from surface modes at short distance [27, 51]. Hence the resonant contribution and the static one are of the same order, as can be seen in the numerical evaluation of the resonant dressing potential at very small atom-surface separations given in Fig. 6. The plot also demonstrates that the asymptotic results of this section (dots) are in excellent agreement with the full calculation based on Eq.(29). From Eq. (33), it is clear that the dynamic atom-surface potential decays on a time scale set by the spectral width $\gamma/2$ of

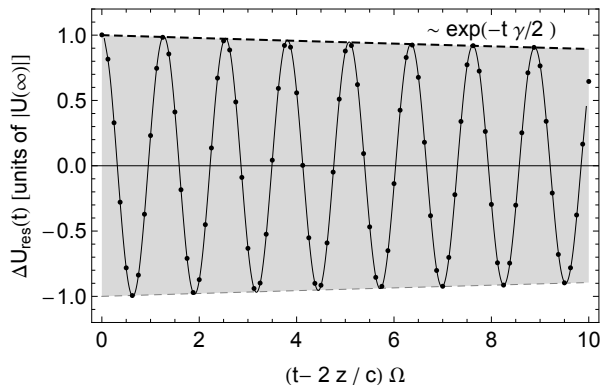


FIG. 6: Dynamic dressing potential after the signal-transit time in the near field ($z = 0.01c/\Omega$) for an initially bare atom. The surface is described by a Drude model for gold with parameters as in Fig. 1 and the atomic transition corresponds to 780nm. The grey envelope shows the exponential damping with a rate $\gamma/2$. The solid curve corresponds to the numerical evaluation of Eqs. (29) and (28), and the surface modes for the lossy Drude model. Dots indicate the asymptotic result of Eq. (33).

the surface plasmon mode. This is at variance with the result in the far field, where the slope of the dispersion relation was the reason for the relaxation. As another immediate consequence, the resonant potential oscillates at a frequency $\Omega + \omega_{\text{sp}}$. Again, this differs completely from the far-field result, where the oscillation is basically given by the atomic transition frequency [see Eq. (29)].

III. PARTIAL DRESSING AFTER A NONADIABATIC TRANSITION

We now consider the case when the atom-surface system is in a fully relaxed or dressed state and some system parameter is suddenly changed. We call this scenario ‘partial dressing’. This has been considered in Ref. [25] for an atom near a perfect reflector. Also, the time evolution of the Casimir-Polder force between two neutral atoms starting from a partially dressed state of the system has been investigated in [52].

We denote $|G\rangle$ the fully-dressed atomic ground state. This state is obtained by perturbation expansion in the basis of the uncoupled Hamiltonian. At first order in the coupling constant

$$|G\rangle = |\text{vac}, \downarrow\rangle + |\{1\}, \uparrow\rangle, \quad (34)$$

$$\begin{aligned} |\{1\}, \uparrow\rangle &= \sum_{|\Psi\rangle \neq |\text{vac}, \downarrow\rangle} \frac{\langle \Psi | H_{AF} | \text{vac}, \downarrow \rangle}{E_{\Psi} - E_0} |\Psi\rangle \\ &= -id_m \int_0^{\infty} d\omega \int d^3\mathbf{x} \sqrt{\frac{\varepsilon_0}{\pi\hbar}} \text{Im} \varepsilon(\mathbf{x}, \omega) \\ &\quad \times \frac{\mathcal{G}_{mn}^*(\mathbf{r}, \mathbf{x}, \omega)}{\omega + \Omega} f_n^\dagger(\mathbf{x}, \omega) |\text{vac}, \uparrow\rangle. \end{aligned} \quad (35)$$

The sum over possible elements $f_n^\dagger |\text{vac}, \uparrow\rangle$ corresponds to the cloud of virtual bosons surrounding the atom. Note that $\langle G | G \rangle = 1 + \mathcal{O}(d_m d_n)$ so that normalization corrections result subleading and the dressed state may be considered normalized in the following.

We now suppose that the system is in the stationary state $|G\rangle$ and that a nonadiabatic (i.e. instantaneous) change in a system parameter occurs at $t = 0$. In the following, the new system observables are marked with a tilde. To begin with, we consider a change of the atomic transition frequency $\Omega \rightarrow \tilde{\Omega}$ which might be induced by the sudden onset of an external electric field via the Stark shift. This transition does not affect the matter-assisted field part of the system and leaves the structure of the Hilbert space unaltered. The rapidity of the transition makes sure that the quantum state immediately after $t = 0$ remains otherwise the same as before.

The dynamic Casimir-Polder potential is then calculated in the Heisenberg picture

$$\begin{aligned} \tilde{U}(z, t) &= \frac{1}{2} \langle G | \tilde{H}_{AF}(t) | G \rangle \quad (36) \\ &= \frac{1}{2} \langle \text{vac}, \downarrow | \tilde{H}_{AF}(t) | \text{vac}, \downarrow \rangle \\ &\quad + \frac{1}{2} \left(\langle \text{vac}, \downarrow | \tilde{H}_{AF}(t) | \{1\}, \uparrow \rangle + \text{c.c.} \right) \\ &\quad + \frac{1}{2} \langle \{1\}, \uparrow | \tilde{H}_{AF}(t) | \{1\}, \uparrow \rangle. \end{aligned} \quad (37)$$

Evaluation up to second order in the dipole moment is again sufficient for our purposes. The first term of Eq. (37) mirrors Eq. (11) and recovers the form of Eq. (15), $\tilde{U}_{\text{stat}} + \tilde{U}_{\text{dyn}}$, with the old transition frequency replaced by the new one. The third term is a higher-order contribution and, hence, neglected here. Finally, the second term yields a correction $\Delta\tilde{U}_p$ that is unique to the partial-dressing scenario. The partial dressing dynamics is hence described by the total time-dependent potential

$$\tilde{U}(z, t) = \left[\tilde{U}_{\text{stat}}(z) + \tilde{U}_{\text{dyn}}(z, t) \right] + \Delta\tilde{U}_p(z, t), \quad (38)$$

where the partial dressing correction is

$$\begin{aligned} \Delta\tilde{U}_p(z, t) &= -\text{Re} \langle \text{vac}, \downarrow | \hat{\mathbf{d}}^{(0)} \cdot \mathbf{E}^{(0)} | \{1\}, \uparrow \rangle \\ &= -d_m d_n \text{Re} \int_0^{\infty} \frac{d\omega}{2\pi} \frac{2e^{-i(\omega + \tilde{\Omega})t}}{\omega + \tilde{\Omega}} \\ &\quad \times \int d^3\mathbf{x} \varepsilon_0 \text{Im} \varepsilon(\mathbf{x}, \omega) \\ &\quad \times \mathcal{G}_{ml}(\mathbf{r}, \mathbf{x}, \omega) \mathcal{G}_{nl}^*(\mathbf{r}, \mathbf{x}, \omega). \end{aligned} \quad (39)$$

As before, the spatial integral in Eq. (39) can be performed using Eq. (12). This gives the concise expression

$$\begin{aligned} \tilde{U}(z, t) &= - \int_0^{\infty} \frac{d\omega}{2\pi} \text{Im} [G(z, \omega)] \quad (40) \\ &\quad \times \left[\frac{2}{\tilde{\Omega} + \omega} - \frac{2 \cos[(\tilde{\Omega} + \omega)t]}{\tilde{\Omega} + \omega} + \frac{2 \cos[(\tilde{\Omega} + \omega)t]}{\Omega + \omega} \right], \end{aligned}$$

using again the shorthand $G(z, \omega)$ defined in Eq.(16) above. The fractions in brackets correspond to the three

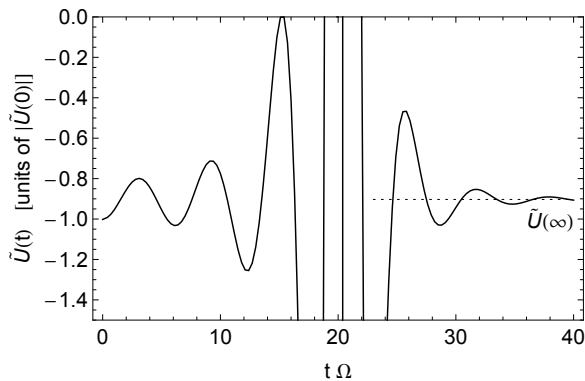


FIG. 7: Partial dressing starting from a dressed ground state, after a sudden change in the atomic transition $\Omega \rightarrow \tilde{\Omega}$. The new transition $\tilde{\Omega} = 0.9\Omega$ corresponds a wavelength 780 nm and the surface is described by a Drude model for gold with parameters as in Fig. 1. The energy just after the non adiabatic transition, $\tilde{U}(0)$ is the same as in the dressed ground state before. The divergence occurs around the signal-transit time $2z/c$. A large distance $z = 10c/\Omega$ is considered. The value of the new static shift $\tilde{U}(\infty)$ can be understood from the $1/\tilde{\Omega}$ scaling of the static polarizability [39].

terms in Eq.(38). The mathematical structure shows immediately how this potential connects the old stationary state ($t = 0$, provided by the last term) and the new one ($t \rightarrow \infty$, first term). This is also clearly visible in Fig. 7 which presents the time-dependent potential during the partial dressing. In the far-field situation considered here, the surface modes do not contribute strongly and the results resemble those obtained in the case of a perfect reflector [25]. The latter limit can be recovered analytically from Eqs. (40) and (18).

The partial dressing interaction can be analyzed along the lines of Sec.II, considering separately the plasmon-pole contribution (contour III in Fig.2) and the nonresonant one [imaginary-frequency integrals in Eq.(23)]. Fig. 8(a) shows the results for the same Stark shift as in Fig. 7, but at short distance. Parameters are chosen such that the terms in brackets in Eq. (38) coincide with the curve shown in Fig. 6. The partial dressing correction $\Delta\tilde{U}_p$ is comparable in amplitude to these terms, but carries the opposite sign. The total potential after the frequency shift oscillates around the new static value with a reduced amplitude as shown in Fig. 8(b).

A closely related scenario involves a change in the transition dipole $\mathbf{d} \rightarrow \tilde{\mathbf{d}}$. This can occur, e.g., if an external field induces a sudden (orientation) polarization of the atom. The dynamic Casimir-Polder potential is obtained as before and results in a slightly different formula where the partial dressing correction depends on both the old

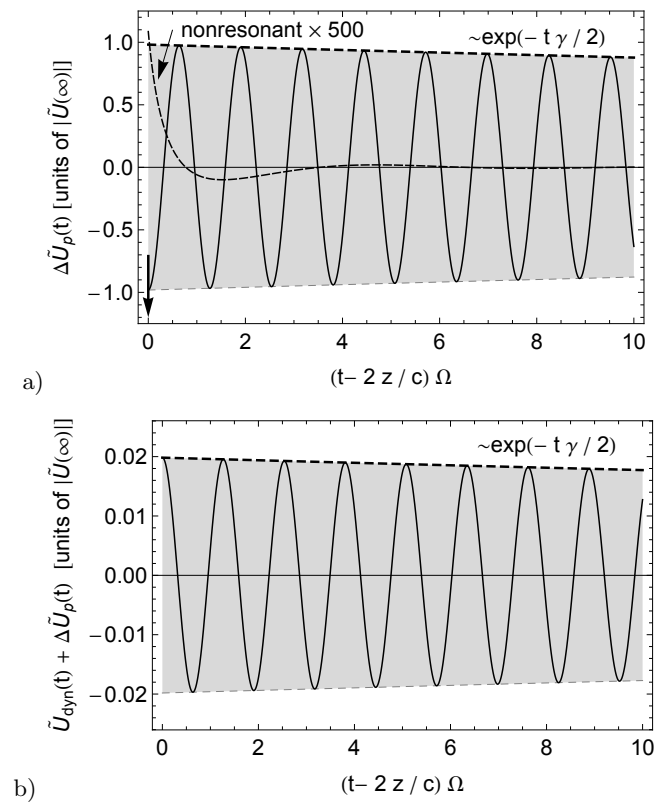


FIG. 8: a) Partial dressing correction $\Delta\tilde{U}_p(t)$ after the signal-transit time in the near field ($z = 0.01c/\Omega$) after the atomic transition is shifted so that the new value $\tilde{\Omega} = 0.9\Omega$ corresponds to the transition wavelength 780nm. The surface is described by a Drude model for gold with parameters as in Fig. 1. The grey envelope shows the exponential damping with a rate $\gamma/2$. The dashed curve shows the nonresonant contribution to the partial dressing potential and has been multiplied by a factor 500 for visibility. b) Total time-dependent contribution to the partial dressing potential in the same scenario. At the distance and parameters chosen, the contribution $\tilde{U}_{\text{dyn}} = U_{\text{dyn}}|_{\Omega \rightarrow \tilde{\Omega}}$ coincides with the curve given in Fig. 6. According to Eq. (38), the two contributions must be added up, resulting in a reduced amplitude of the plasmonic oscillations.

and the new dipole moment

$$\tilde{U}(z, t) = \tilde{U}_{\text{stat}}(z) + \tilde{d}_m(\tilde{d}_n - d_n) \times \int_0^\infty \frac{d\omega}{\pi} \text{Im} [\mathcal{G}_{mn}(\omega)] \frac{\cos[(\Omega + \omega)t]}{\Omega + \omega}. \quad (41)$$

In this case, there is a discontinuity in the potential at $t = 0$. This is indeed expected from a physical point of view, because the interaction energy between the atom and the local field at its position is immediately affected by the change in the atomic dipole. When $\mathbf{d} \cdot \tilde{\mathbf{d}} \ll |\tilde{\mathbf{d}}|^2$ (by amplitude or orientation), the partial dressing correction is negligible. This agrees with the intuitive notion of “switching on the interaction” in the bare atomic dressing of Sec. I.

IV. SUMMARY AND DISCUSSION

The dynamic atom-surface Casimir-Polder interaction has been investigated from the perspective of atomic self-dressing for an initially bare or partially dressed atom near a surface described by general optical reflection coefficients. In the more realistic scenario of a partially dressed state, the system relaxes after a sudden change in the atomic transition frequency or the transition dipole. We have thus generalized previous work on dynamic Casimir-Polder interaction [24, 25] with perfectly reflecting surfaces to more realistic ones using the quantization scheme for matter-assisted fields to include boundaries with, in principle, arbitrary dielectric or magnetic properties. Although the limit of perfectly reflecting surfaces can be often considered as a reasonable approximation in the radiative zone, that is for distances far beyond the atomic transition wavelengths, many interesting phenomena require a more detailed surface model, in particular when shorter distances are considered. This is not unexpected, because surface excitations are known to dominate the response in the near-field zone [28–32].

Within this framework, we have studied the dynamic dressing and the consequent dynamic Casimir-Polder potential between a two-level atom and a surface in different nonequilibrium situations: an initially bare ground-state atom and a partially dressed atom. We have compared the results obtained using parameters typical of a gold surface (Drude model) with recent results in the literature obtained for a perfectly reflecting surface and isolated the resonant surface-mode contributions to the time-dependent atom-surface potential in different distance regimes. Far from the surface, this contribution is a minor correction to the dynamic atom-surface potential and decays quickly ($\propto t^{-5}$) due to the dephasing of different frequency components. In contrast, at short distances the dynamic Casimir-Polder interaction bears the characteristics of a transient excitation of the surface plasmon modes that dominate the response by orders of magnitude and decays on a much slower scale related to the electron scattering time in the bulk metal. Both for the initially bare atom and for the partially dressed one, we have found that time intervals exist where the Casimir-Polder potential is repulsive. The particular case of an atom dressing after a change in its transition dipole moment may effectively provide a realization of the bare dressing scenario.

Our formalism may be immediately generalized to other types of emitters such as small molecules, quantum dots, Rydberg states, or – in analogy to the dynamic Casimir effect studied in Ref. [20] – superconducting flux qubits. Among these, the latter two feature a considerable magnetic polarizability, leading to a high sensitivity towards the low-frequency electromagnetic modes [45, 48, 49]. A study of such systems would contribute to the understanding of the role of the DC conductivity in the macroscopic Casimir interaction [53, 54]. A particularly interesting scenario could be the partial dress-

ing triggered by a phase transition in the surface which quickly changes the optical properties, e.g. in the evolution of a magnetic dipole close to a superconductor near criticality. Knowledge of the atomic response to a perturbation of superconductivity is also relevant for experiments with superconducting atom chips [55]. In this case, the formalism of Sec. III must be amended to ensure a fully retarded signal at the dipole position.

Finally, the thermal occupation of the field and surface modes [56] may affect the dynamic dressing. Thermal excitations can be absorbed by the atom, giving rise to additional resonant contributions. The width of the thermal spectrum is likely to introduce a characteristic time scale $\hbar/k_B T \approx 1 \text{ ps} \times (T/1\text{K})^{-1}$. If thermal occupation of excited atomic states is relevant, spontaneous emission will play a role in the dynamic Casimir-Polder interaction. The study of dressing may thus give some insight into the process of thermalization.

Acknowledgments

Partial financial support by Deutscher Akademischer Austauschdienst (grant D/10/41486), the German-Israeli Foundation for Scientific Research and Development, by the Julian Schwinger Foundation, by MIUR, and by Comitato Regionale di Ricerche Nucleari e di Struttura della Materia is gratefully acknowledged. The authors also acknowledge support from the ESF Research Networking Program CASIMIR and thank R. Messina and F. Intravaia for helpful discussions.

Appendix A: Electric Green's tensor

The retarded electric Green's tensor describes the electric field

$$E_i(\mathbf{x}, \omega) = \mathcal{G}_{ij}(\mathbf{x}, \mathbf{r}, \omega) d_j(\omega) \quad (\text{A1})$$

radiated by a point-like fictitious dipole source \mathbf{d} placed in \mathbf{r} . Note that other authors use a different normalization for the Green tensor; in Refs. [35–39], a prefactor $\omega^2/(\epsilon_0 c^2)$ would appear in Eq. (A1).

Near a single surface, this field consists of a free-space part and a reflected contribution $\mathcal{G} = \mathcal{G}^{\text{free}} + \mathcal{G}^{\text{refl}}$. We concentrate in this work on the reflected field contributions, that dominate the imaginary part of the Green's tensor by far at short distances. Neglecting the free space contribution also provides a convenient way of removing the formally diverging Lamb shift from the interaction potentials [43].

The general expression for the reflected (retarded) Green's tensor can be conveniently expressed in the Weyl basis of transverse s- and p-polarized waves, also known as TE- and TM-polarization, respectively [57]. For a local, isotropic, nonmagnetic bulk medium, the reflection

coefficients read

$$r_s(\omega, p) = \frac{\kappa - \kappa_m}{\kappa + \kappa_m}, \quad r_p(\omega, p) = \frac{\varepsilon(\omega)\kappa - \kappa_m}{\varepsilon(\omega)\kappa + \kappa_m}, \quad (\text{A2})$$

where $\kappa = \sqrt{p^2 - \omega^2/c^2}$ and $\kappa_m = \sqrt{p^2 - \varepsilon(\omega)\omega^2/c^2}$

($\text{Re } \kappa \geq 0, \text{Im } \kappa \leq 0$ for $\omega > 0$) are the propagation constants in vacuum and inside the bulk. In the limit $\mathbf{x} \rightarrow \mathbf{r}$, we obtain the single-point reflected Green's tensor, which depends only on the distance z from the surface (SI units)

$$\mathcal{G}_{ij}^{\text{refl}}(z, \omega) = \frac{1}{8\pi\varepsilon_0} \int_0^\infty \frac{p}{\kappa} dp e^{-2\kappa z} \left[\left(\kappa^2 r_p(\omega, p) + \frac{\omega^2}{c^2} r_s(\omega, p) \right) [\delta_{ij} - \hat{z}_i \hat{z}_j] + 2p^2 r_p(\omega, p) \hat{z}_i \hat{z}_j \right]. \quad (\text{A3})$$

From this expression, the limit of an ideally reflecting surface of Eq. (18) can be obtained by setting $r_p = -r_s \rightarrow 1$. For an isotropic polarizability, only the trace of the tensor is required.

Note finally, that at very short distances from the surface, high values of $p \gg \omega/c$ dominate the inte-

gral so that $\kappa, \kappa_m \approx p$. Here, the reflection coefficients are approximated by $r_p \approx [\varepsilon(\omega) - 1]/[\varepsilon(\omega) + 1]$, $r_s \approx (\varepsilon(\omega) - 1)\omega^2/(4c^2 p^2)$. The s-polarized contribution to the Green's tensor is suppressed by a factor $\omega^2/(cp)^2$ and can be neglected. This gives the near field limit of Eq. (30).

-
- [1] P.W. Milonni, *The Quantum Vacuum: An Introduction to Quantum Electrodynamics*, Academic Press (San Diego, 1994).
- [2] G. Compagno, R. Passante, F. Persico, *Atom-Field Interactions and Dressed Atoms*, Cambridge University Press (Cambridge, 1995).
- [3] *Casimir Physics*, edited by D. Dalvit, P. W. Milonni, D. Roberts, F.S.S. Rosa, (Springer, Heidelberg, 2011).
- [4] M. Bordag, G. L. Klimchitskaya, U. Mohideen, V.M. Mostepanenko *Advances in the Casimir Effect*, Oxford Science Publications (2011).
- [5] H.B.G. Casimir, D. Polder, Phys. Rev. **73**, 360 (1948).
- [6] D.P. Craig, T. Thirunamachandran, *Molecular Quantum Electrodynamics*, Dover (1998).
- [7] R. Messina, R. Passante, L. Rizzuto, S. Spagnolo, R. Vasile, J. Phys. A **41**, 164031 (2008) and references therein.
- [8] H. B. G. Casimir, Proc. kon. Ned. Ak. Wet **51**, 793 (1948).
- [9] E. A. Power and T. Thirunamachandran, Phys. Rev. A **50**, 3929 (1994).
- [10] R. Messina and R. Passante, Phys. Rev. A **76**, 032107 (2007).
- [11] V. Sandoghdar, C. I. Sukenik, E. A. Hinds, S. Haroche, Phys. Rev. Lett. **68**, 3432 (1992).
- [12] C. I. Sukenik, M. G. Boshier, D. Cho, V. Sandoghdar, E. A. Hinds, Phys. Rev. Lett. **70**, 560 (1993).
- [13] F. M. Serry, D. Walliser, G.J. Maclay, J. Appl. Phys. **84**, 2501 (1998).
- [14] R. Salem, Y. Japha, J. Chabé, B. Hadad, M. Keil, K. A. Milton, and R. Folman, New J. Phys. **12**, 023039 (2010).
- [15] V. V. Dodonov, Physica Scripta **82**, 038105 (2010).
- [16] C. Braggio, G. Bressi, G. Carugno, C. Del Noce, G. Galeazzi, A. Lombardi, A. Palmieri, G. Ruoso, D. Zanello, Europhys. Lett. **70**, 754(2005).
- [17] V. V. Dodonov, A. V. Dodonov, J. Phys. B **39**, S749 (2006).
- [18] V. V. Dodonov, A. V. Dodonov, J. Phys. A **39**, 6271(2006).
- [19] F. X. Dezael and A. Lambrecht, Europhys. Lett. **89**, 14001 (2010).
- [20] J.R. Johansson, G. Johansson, C.M. Wilson, F. Nori, Phys. Rev. Lett. **103**, 147003 (2009).
- [21] J.C. Jausula, G.B. Partridge, M. Bonneau, R. Lopes, J. Ruau del, D. Boiron, and C.I. Westbrook, Phys. Rev. Lett. **109**, 220401 (2012).
- [22] P.O. Westlund and H. Wennerström, Phys. Rev. A **71**, 062106 (2005).
- [23] S. Shresta, B.L. Hu, N.G. Phillips, Phys. Rev. A **68**, 062101 (2003).
- [24] R. Vasile, R. Passante, Phys. Rev. A **78**, 032108 (2008).
- [25] R. Messina, R. Vasile, R. Passante, Phys. Rev. A **82**, 062501 (2010).
- [26] N. Bartolo, R. Passante, Phys. Rev. A **86**, 012122 (2012).
- [27] J. F. Annett and P. M. Echenique, Phys. Rev. B, **34**, 6853 (1986).
- [28] G.W. Ford, W.H. Weber, Phys. Rep. **113**, 195 (1984).
- [29] H. Failache, S. Saltiel, A. Fischer, D. Bloch, M. Ducloy, Phys. Rev. Lett. **88**, 243603 (2002).
- [30] C. Henkel, K. Joulain, J.-P. Mulet, J.-J. Greffet, J. Opt. A **4**, S109 (2002).
- [31] M.P. Gorza, M. Ducloy, Eur. Phys. J. D **40**, 343 (2006).
- [32] C. Stehle, H. Bender, C. Zimmermann, D. Kern, M. Fleischer, S. Slama, Nat. Photon. **5**, 494 (2011).
- [33] E.L. Feinberg, Sov. Phys. JETP **23**, 132 (1966) [J. Exptl. Theor. Phys. (USSR) **50**, 202]. (1966)]; Sov. Phys. USP **23**, 629 (1981) [Usp. Fiz. Nauk. **132**, 255 (1981)].
- [34] R. Passante and N. Vinci, Phys. Lett. A **213**, 119 (1996).
- [35] L. Knöll, S. Scheel, D.-G. Welsch, in J. Perina (ed.) *Coherence and Statistics of Photons and Atoms*, Wiley (New York, 2001).
- [36] H. Safari, S.Y. Buhmann, D.-G. Welsch, H.T. Dung, Phys. Rev. A **74**, 042101 (2006).
- [37] S.Y. Buhmann, D.-G. Welsch, Progr. Quant. Electron.

- 31**, 51 (2007).
- [38] S. Scheel, S.Y. Buhmann, *Acta Phys. Slov.* **58**, 675 (2008).
- [39] S. Y. Buhmann, *Dispersion Forces I – Macroscopic Quantum Electrodynamics and Ground-State Casimir, Casimir–Polder and van der Waals Forces*, Springer Tracts in Modern Physics, vol. 247 (Springer, Heidelberg, 2012).
- [40] The approximation of a nonmagnetic material neglects possible E - B -cross-correlations. The generalization to arbitrary magnetodielectrics is straightforward, see for example Ref. [36]. However, this brings along a more involved notation, and we restrict the present analysis to purely dielectric materials for clarity.
- [41] W. Eckhardt, *Physica A* **82**, 128 (1984).
- [42] H.T. Dung, L. Knöll, D.-G. Welsch, *Phys. Rev. A* **57**, 3931 (1998).
- [43] J.M. Wylie, J.E. Sipe, *Phys. Rev. A* **32**, 2030 (1985).
- [44] P.W. Milonni, *Phys. Rep.* **25**, 1 (1976).
- [45] H.R. Haakh, F. Intravaia, C. Henkel, S. Spagnolo, R. Passante, B. Power, F. Sols, *Phys. Rev. A* **80**, 062905 (2009).
- [46] F. Flores, F. García-Moliner, *Introduction to the Theory of Solid Surfaces*, Cambridge University Press (1979).
- [47] H. Raether, *Surface Plasmons on Smooth and Rough Surfaces and on Gratings*, Springer, 1988.
- [48] F. Intravaia, C. Henkel, *Phys. Rev. Lett.* **103**, 130405 (2009).
- [49] F. Intravaia, S. A. Ellingsen, C. Henkel, *Phys. Rev. A* **82**, 032504 (2010).
- [50] K. Joulain, J.-P. Mulet, F. Marquier, R. Carminati, J.-J. Greffet, *Surf. Science Rep.* **57**, 59 (2005).
- [51] A. Zangwill, *Physics at Surfaces* (Cambridge University Press, Cambridge, 1988).
- [52] R. Passante, F. Persico, *Phys. Lett. A* **312**, 319 (2003).
- [53] G. Bimonte, E. Calloni, G. Esposito, L. Milano, and L. Rosa, *Phys. Rev. Lett.* **94**, 180402 (2005).
- [54] G. Bimonte, H. R. Haakh, C. Henkel, F. Intravaia, *J. Phys A* **43**, 145304 (2010).
- [55] J. Reichel, V. Vuletic (eds.), *Atom Chips*, Wiley-VCH (2011).
- [56] S. Ribeiro, S. Y. Buhmann, and S. Scheel, *Phys. Rev. A* **87**, 042508 (2013).
- [57] J.E. Sipe, *Surf. Science* **105**, 489 (1981).